Eur. Phys. J. E **28**, 139–146 (2009)
DOI 10.1140/epje/i2008-10363-x

THE EUROPEAN PHYSICAL JOURNAL E

Regular Article

Dynamical density functional theory for colloidal dispersions including hydrodynamic interactions

M. Rex[a] and H. Löwen

Institut für Theoretische Physik II: Weiche Materie, Heinrich-Heine-Universität Düsseldorf, Universitätsstraße 1, D-40225 Düsseldorf, Germany

Received 11 June 2008 and Received in final form 24 July 2008
Published online: 16 September 2008 –

Abstract. A dynamical density functional theory (DDFT) for translational Brownian dynamics is derived which includes hydrodynamic interactions. The theory reduces to the simple Brownian DDFT proposed by Marconi and Tarazona (U. Marini Bettolo Marconi and P. Tarazona, J. Chem. Phys. **110**, 8032 (1999); J. Phys.: Condens. Matter **12**, A413 (2000)) when hydrodynamic interactions are neglected. The derivation is based on Smoluchowski's equation for the time evolution of the probability density with pairwise hydrodynamic interactions. The theory is applied to hard-sphere colloids in an oscillating spherical optical trap which switches periodically in time from a stable confining to an unstable potential. Rosenfeld's fundamental measure theory for the equilibrium density functional is used and hydrodynamics are incorporated on the Rotne-Prager level. The results for the time-dependent density profiles are compared to extensive Brownian dynamics simulations which are performed on the same Rotne-Prager level and excellent agreement is obtained. It is further found that hydrodynamic interactions damp and slow the dynamics of the confined colloid cluster in comparison to the same situation with neglected hydrodynamic interactions.

PACS. 82.70.Dd Colloids – 61.20.Ja Computer simulation of liquid structure – 64.70.D- Solid-liquid transitions – 05.70.Ln Nonequilibrium and irreversible thermodynamics

1 Introduction

The dynamics of colloidal particles dispersed in a molecular solvent is by far less understood than their static behavior. The reason is that colloidal dynamics span a wide range of time scales due to the enormous difference in size and mass of the colloidal particles and the host solvent molecules [1]. The obvious approach to this problem is to reduce the description of the solvent, when one is interested in the dynamics of the colloidal particles alone. While in equilibrium all solvent effects can be mapped on an effective interaction potential between the colloids [2,3], in nonequilibrium additional solvent effects need to be taken into account. These are: the friction of the colloids with the solvent, their Brownian motion due to random kicks of the solvent molecules, and solvent-flow–mediated interactions, the so-called hydrodynamic interactions. This is either done by solving Langevin's equations of motion for the constituent particles, or —equivalently— by describing the time evolution of the probability density in configurational space with the Smoluchowski equation [4,5]. The former description takes the Brownian motion of the particles explicitly into account and builds the basis of Brownian dynamics computer simulations.

Though a full microscopic theory for the time evolution of the probability density including hydrodynamic interactions through the mobility tensor is in principle given by the Smoluchowski equation, the many-body nature of the problem and the long range of the Oseen mobility tensor which is the leading contribution for a colloidal pair are making the elaboration of reliable approximations difficult. Explicit approaches have been worked out in the bulk for short-time and long-time diffusion coefficients [6–10], and for the viscosity [11]. There are also first investigations for colloids near walls and on interfaces [12,13] and for the nonequilibrium structure of colloids [14] but a general theory for an arbitrary and time-dependent inhomogeneous external potential is missing.

A promising approach to describing the dynamics of colloidal particles is a dynamical density functional theory (DDFT) which generalizes the classical equilibrium density functional theory (DFT) towards nonequilibrium situations. The standard equilibrium density functional approach is a microscopic theory which starts from the interparticle interactions and bulk fluid correlations as an

[a] e-mail: rexm@thphy.uni-duesseldorf.de

input. It predicts the inhomogeneous density profiles in an external potential including strongly inhomogeneous situations like freezing, for reviews see [15–17]. The key quantity is the excess ("over ideal-gas") free-energy density functional, which is in general unknown. However, to date very accurate approximations for various interparticle interactions are available. For example, Rosenfeld's fundamental measure theory [18,19] has been shown to be very reliable for hard spheres, and the mean-field approximation is asymptotically correct for soft-core interaction at high densities [20–22].

While it is by now well understood how to extract the static equilibrium properties of an inhomogeneous system from density functional theory, its extension toward time-dependent dynamical situations in nonequilibrium is more challenging. Recently, a DDFT was developed [23–25] where hydrodynamic interactions are ignored. DDFT results for the nonequilibrium dynamics of inhomogeneous Brownian fluids were found to agree very well with simulation data [26–28]. Further important activities in developing the dynamical extension of DFT lie in the existence proof of the dynamical functional [29], its applicability to Newtonian dynamics [30] and to include fluctuations and noise effects [31]. Still lacking to date is how hydrodynamic interactions are to be treated in the DDFT formalism. Some attempts have been carried out by including hydrodynamic interaction effects in an effective way in a density-dependent diffusion coefficient [32]. Here, we present a stringent derivation of a DDFT which takes hydrodynamic interactions on a two-particle level into account without making further approximations than those underlying the DDFT of Marconi and Tarazona [23,24].

This theory is then applied to the dynamics of hard-sphere colloids confined in a time-dependent oscillating spherical cavity. Hydrodynamic interactions are incorporated on the pairwise Rotne-Prager level and Rosenfeld's fundamental measure theory for the hard-sphere equilibrium density functional is used. The results are compared to Brownian dynamics computer simulations, performed on the same level of approximation for the hydrodynamic interactions, and excellent agreement is found. When compared to reference calculations where hydrodynamic interactions are neglected, it is found the their inclusion leads to a significant damping of the oscillations in the steady-state density profiles of hard spheres in a oscillating trap. We further compare our results to those obtained when using a density-dependent diffusion coefficient as proposed by Royall *et al.* [32]. This latter approach yields better agreement than that without hydrodynamic interactions but not than that with hydrodynamic interactions. A previous account of some of the results of this paper was published elsewhere [33].

This paper is laid out as follows. In Section 2, starting from the Smoluchowski equation, we derive a generalized dynamical density functional theory which includes hydrodynamic interactions. Section 3 is devoted to describing the system and the associated free-energy functional. In Section 4 we present the results obtained by DDFT and Brownian dynamics simulations. Finally, in Section 5 we draw some conclusions.

2 Equation of motion for the one-body density

In this section we derive a functional theory that predicts the time evolution of the one-body density $\rho(\mathbf{r},t)$ including hydrodynamic interactions. We start from the equation for the time evolution of the full probability density distribution $P(\mathbf{r}^N,t)$ for N interacting spherical Brownian particles at positions $\mathbf{r}^N=\mathbf{r}_1,\mathbf{r}_2,\ldots,\mathbf{r}_N$ and at time t, *i.e.*, the Smoluchowski equation (see, *e.g.*, [5])

$$\frac{\partial P(\mathbf{r}^N,t)}{\partial t}= \sum_{i,j}^{N}\boldsymbol{\nabla}_i\cdot\mathbf{D}_{ij}(\mathbf{r}^N)\cdot\left[\boldsymbol{\nabla}_j+\frac{\boldsymbol{\nabla}_j U(\mathbf{r}^N,t)}{k_{\mathrm{B}}T}\right]P(\mathbf{r}^N,t). \quad (1)$$

$k_{\mathrm{B}}T$ is the thermal and $U(\mathbf{r}^N,t)$ the total potential energy of the system. By using the Smoluchowski equation, the description of the complex fluid is reduced to one based solely on the position coordinates of the colloids, rather than utilizing the full set of phase space coordinates for the colloid and solvent particles. The solvent-mediated hydrodynamic interactions are thereby included through the configuration-dependent diffusion tensor $\mathbf{D}_{ij}(\mathbf{r}^N)$. In our approach, we approximate the diffusion tensor on a two-particle level: $\mathbf{D}_{ij}(\mathbf{r}^N)\approx D_0\mathbf{1}\delta_{ij}+\mathbf{D}_{ij}^{(2)}(\mathbf{r}^N)$, which is in general only justified for small volume fractions of the colloidal particles. D_0 denotes the diffusion constant of a single isolated particle, δ_{ij} is Kronecker's delta, and

$$\mathbf{D}_{ij}^{(2)}(\mathbf{r}^N)=D_0\left[\delta_{ij}\sum_{l\neq i}^{N}\boldsymbol{\omega}_{11}(\mathbf{r}_i-\mathbf{r}_l)+(1-\delta_{ij})\boldsymbol{\omega}_{12}(\mathbf{r}_i-\mathbf{r}_j)\right]. \quad (2)$$

Series expansions of the two tensors $\boldsymbol{\omega}_{11}$ and $\boldsymbol{\omega}_{12}$ are known to arbitrary order [34]. We further assume pairwise additivity for the total potential energy of the system, such that $U(\mathbf{r}^N,t)$ reads as

$$U(\mathbf{r}^N,t)=\sum_{m=1}^{N}V_{\mathrm{ext}}(\mathbf{r}_m,t)+\frac{1}{2}\sum_{m=1}^{N}\sum_{n\neq m}^{N}v_2(\mathbf{r}_m,\mathbf{r}_n), \quad (3)$$

where $V_{\mathrm{ext}}(\mathbf{r},t)$ is the one-body time-dependent external potential acting on each particle and $v_2(\mathbf{r}_i,\mathbf{r}_j)$ is the pair potential. The latter is assumed to be time-independent. To obtain an equation for the time evolution of the one-body density, we note that the n-body densities are given by integrals over the probability density [25]

$$\rho^{(n)}(\mathbf{r}^n,t)=\frac{N!}{(N-n)!}\int \mathrm{d}\mathbf{r}_{n+1}\ \ldots\int \mathrm{d}\mathbf{r}_N\ P(\mathbf{r}^N,t). \quad (4)$$

Thus, by integrating equation (1) with $N\int \mathrm{d}\mathbf{r}_2\ \ldots\int \mathrm{d}\mathbf{r}_N$, we obtain the following equation for the one-body density:

$$k_{\mathrm{B}}T/D_0\frac{\partial\rho(\mathbf{r},t)}{\partial t}=\boldsymbol{\nabla}_{\mathbf{r}}\cdot\left\{\mathbf{j}_1+\mathbf{j}_2+\mathbf{j}_3\right\}, \quad (5)$$

with the current densities

$$\mathbf{j}_1 = k_\mathrm{B}T\boldsymbol{\nabla}_\mathbf{r}\rho(\mathbf{r},t) + \rho(\mathbf{r},t)\boldsymbol{\nabla}_\mathbf{r}V_\mathrm{ext}(\mathbf{r},t) + \int \mathrm{d}\mathbf{r}'\ \rho^{(2)}(\mathbf{r},\mathbf{r}',t)\boldsymbol{\nabla}_\mathbf{r}v_2(\mathbf{r},\mathbf{r}'), \tag{6}$$

$$\mathbf{j}_2 = \int \mathrm{d}\mathbf{r}'\ \boldsymbol{\omega}_{11}(\mathbf{r}-\mathbf{r}')\cdot\Big\{k_\mathrm{B}T\boldsymbol{\nabla}_\mathbf{r}\rho^{(2)}(\mathbf{r},\mathbf{r}',t) + \boldsymbol{\nabla}_\mathbf{r}\left[V_\mathrm{ext}(\mathbf{r},t)+v_2(\mathbf{r},\mathbf{r}')\right]\rho^{(2)}(\mathbf{r},\mathbf{r}',t) + \int \mathrm{d}\mathbf{r}''\ \rho^{(3)}(\mathbf{r},\mathbf{r}',\mathbf{r}'',t)\boldsymbol{\nabla}_\mathbf{r}v_2(\mathbf{r},\mathbf{r}'')\Big\}, \tag{7}$$

and

$$\mathbf{j}_3 = \int \mathrm{d}\mathbf{r}'\ \boldsymbol{\omega}_{12}(\mathbf{r}-\mathbf{r}')\cdot\Big\{k_\mathrm{B}T\boldsymbol{\nabla}_{\mathbf{r}'}\rho^{(2)}(\mathbf{r},\mathbf{r}',t) + \boldsymbol{\nabla}_{\mathbf{r}'}[V_\mathrm{ext}(\mathbf{r}',t)+v_2(\mathbf{r},\mathbf{r}')]\rho^{(2)}(\mathbf{r},\mathbf{r}',t) + \int \mathrm{d}\mathbf{r}''\ \rho^{(3)}(\mathbf{r},\mathbf{r}',\mathbf{r}'',t)\boldsymbol{\nabla}_{\mathbf{r}'}v_2(\mathbf{r}',\mathbf{r}'')\Big\}. \tag{8}$$

Equations (6–8) depend on both the time-dependent two-body and three-body densities. Those are obtained, in principle, by integrating again the Smoluchowski equation (see Eq. (4)) but yield equations that depend on higher n-body densities. This is known as the BBGKY-hierarchy. Thus, an appropriate closure is needed to break the hierarchy. Here, we use an approximation first proposed by Marconi and Tarazona [23,24] and cast the current densities into a form involving exclusively the equilibrium free-energy functional $\mathcal{F}[\rho]$. The basic assumption is to identify the out-of-equilibrium n-body densities, $n \geq 2$, with those of an equilibrium system whose one-body density profile is identical. This allows for making use of the following equilibrium theories: static DFT [35] and the Yvon-Born-Green (YBG) relations (see, *e.g.*, [36]). To that end, we regard an out-of-equilibrium system at time $t = t_0$ with an instantaneous density profile $\rho(\mathbf{r},t_0)$, whose time evolution is given by equation (5). From static DFT it is known that every equilibrium density profile $\rho_0(\mathbf{r})$ is brought about by a unique external potential $\Phi_\mathrm{ext}(\mathbf{r})$. Thus, we can identify the out-of-equilibrium instantaneous density with an equilibrium one of a reference system exposed to an accordingly chosen unique external potential $\Phi_\mathrm{ext}(\mathbf{r},t_0) = u(\mathbf{r},t_0) + V_\mathrm{ext}(\mathbf{r},t_0)$, such that $\rho_0(\mathbf{r}) = \rho(\mathbf{r},t_0)$. This holds for every point in time and therefore $\Phi_\mathrm{ext}(\mathbf{r},t)$, the additional potential $u(\mathbf{r},t)$, and the equilibrium reference density $\rho_t(\mathbf{r})$ depend parametrically on time t. In the equilibrium reference system, the following generalized force balance equation holds [35]:

$$\frac{k_\mathrm{B}T\boldsymbol{\nabla}\rho_t(\mathbf{r})}{\rho_t(\mathbf{r})} + \boldsymbol{\nabla}\Phi_\mathrm{ext}(\mathbf{r},t) = -\boldsymbol{\nabla}\frac{\delta\mathcal{F}_\mathrm{exc}[\rho]}{\delta\rho}\bigg|_{\rho=\rho_t(\mathbf{r})}, \tag{9}$$

with the excess free-energy functional $\mathcal{F}_\mathrm{exc}[\rho]$. This equation allows us to determine the gradient of the external potential $\Phi_\mathrm{ext}(\mathbf{r},t)$ and thus the gradient of the unknown additional potential $u(\mathbf{r},t)$ that brings about the reference density. A simple reorganization (recall that $u(\mathbf{r},t)$ is chosen such that $\rho_t(\mathbf{r}) = \rho(\mathbf{r},t)$ at each point in time) yields

$$\boldsymbol{\nabla}u(\mathbf{r},t) = -\boldsymbol{\nabla}\frac{\delta\mathcal{F}[\rho]}{\delta\rho(\mathbf{r},t)} \equiv -\boldsymbol{\nabla}\mu(\mathbf{r},t), \tag{10}$$

with the free-energy density functional

$$\mathcal{F}[\rho] = k_\mathrm{B}T\int \mathrm{d}\mathbf{r}\ \rho(\mathbf{r},t)[\ln(\Lambda^3\rho(\mathbf{r},t)) - 1] + \mathcal{F}_\mathrm{exc}[\rho] + \int \mathrm{d}\mathbf{r}\ \rho(\mathbf{r},t)V_\mathrm{ext}(\mathbf{r},t). \tag{11}$$

Λ denotes the thermal de Broglie wavelength. $\mu(\mathbf{r},t)$ is the local nonequilibrium chemical potential. In the nonequilibrium system, the gradient of the chemical potential is the thermodynamic driving force. $\boldsymbol{\nabla}u(\mathbf{r},t)$ may therefore be envisaged as the additional external force which is necessary to balance the thermodynamic driving force in the equilibrium reference system. In the latter, additionally the YBG-hierarchy holds, whose first two members read [36]

$$\begin{gathered} k_\mathrm{B}T\boldsymbol{\nabla}_\mathbf{r}\rho_t(\mathbf{r}) + \rho_t(\mathbf{r})\boldsymbol{\nabla}_\mathbf{r}\Phi_\mathrm{ext}(\mathbf{r},t) + \int \mathrm{d}\mathbf{r}'\ \rho_t^{(2)}(\mathbf{r},\mathbf{r}')\boldsymbol{\nabla}_\mathbf{r}v_2(\mathbf{r},\mathbf{r}') = 0 \\ \Leftrightarrow \\ -\rho_t(\mathbf{r})\boldsymbol{\nabla}_\mathbf{r}u(\mathbf{r},t) = k_\mathrm{B}T\boldsymbol{\nabla}_\mathbf{r}\rho_t(\mathbf{r}) \\ +\rho_t(\mathbf{r})\boldsymbol{\nabla}_\mathbf{r}V_\mathrm{ext}(\mathbf{r},t) + \int \mathrm{d}\mathbf{r}'\ \rho_t^{(2)}(\mathbf{r},\mathbf{r}')\boldsymbol{\nabla}_\mathbf{r}v_2(\mathbf{r},\mathbf{r}') \end{gathered} \tag{12}$$

and

$$\begin{gathered} \boldsymbol{\nabla}_{\mathbf{r}'}\left[\Phi_\mathrm{ext}(\mathbf{r},t)+v_2(\mathbf{r},\mathbf{r}')\right]\rho_t^{(2)}(\mathbf{r},\mathbf{r}') \\ +k_\mathrm{B}T\boldsymbol{\nabla}_{\mathbf{r}'}\rho_t^{(2)}(\mathbf{r},\mathbf{r}') + \int \mathrm{d}\mathbf{r}''\ \rho_t^{(3)}(\mathbf{r},\mathbf{r}',\mathbf{r}'')\boldsymbol{\nabla}_{\mathbf{r}'}v_2(\mathbf{r}',\mathbf{r}'') = 0 \\ \Leftrightarrow \\ -\rho_t^{(2)}(\mathbf{r},\mathbf{r}')\boldsymbol{\nabla}_{\mathbf{r}'}u(\mathbf{r}',t) = \\ \boldsymbol{\nabla}_{\mathbf{r}'}\left[V_\mathrm{ext}(\mathbf{r}',t)+v_2(\mathbf{r},\mathbf{r}')\right]\rho_t^{(2)}(\mathbf{r},\mathbf{r}') + k_\mathrm{B}T\boldsymbol{\nabla}_{\mathbf{r}'}\rho_t^{(2)}(\mathbf{r},\mathbf{r}') \\ + \int \mathrm{d}\mathbf{r}''\ \rho_t^{(3)}(\mathbf{r},\mathbf{r}',\mathbf{r}'')\boldsymbol{\nabla}_{\mathbf{r}'}v_2(\mathbf{r}',\mathbf{r}''). \end{gathered} \tag{13}$$

The two right-hand sides in the second lines of equations (12) and (13) occur in the dynamical (nonequilibrium) context, equations (6–8). The basic assumption now, which also underlies the original version of the DDFT [23–25], is to use these expressions in the nonequilibrium situation, *i.e.*, we approximate the two-body and three-body densities by those of the reference system with the same one-body density: $\rho^{(2)}(\mathbf{r},\mathbf{r}',t) \approx \rho_t^{(2)}(\mathbf{r},\mathbf{r}')$ and $\rho^{(3)}(\mathbf{r},\mathbf{r}',\mathbf{r}'',t) \approx \rho_t^{(3)}(\mathbf{r},\mathbf{r}',\mathbf{r}'')$. Inserting equations (10, 12), and (13) into equation (5), we obtain

our central result

$$k_{\mathrm{B}}T/D_0\frac{\partial\rho(\mathbf{r},t)}{\partial t} = \boldsymbol{\nabla}_{\mathbf{r}}\Bigg\{\underbrace{\rho(\mathbf{r},t)\boldsymbol{\nabla}_{\mathbf{r}}\frac{\delta\mathcal{F}[\rho]}{\delta\rho(\mathbf{r},t)}}_{\mathbf{j}_1} + \underbrace{\int \mathrm{d}\mathbf{r}'\,\rho^{(2)}(\mathbf{r},\mathbf{r}',t)\boldsymbol{\omega}_{11}(\mathbf{r}-\mathbf{r}')\cdot\boldsymbol{\nabla}_{\mathbf{r}}\,\frac{\delta\mathcal{F}[\rho]}{\delta\rho(\mathbf{r},t)}}_{\mathbf{j}_2} + \underbrace{\int \mathrm{d}\mathbf{r}'\,\rho^{(2)}(\mathbf{r},\mathbf{r}',t)\boldsymbol{\omega}_{12}(\mathbf{r}-\mathbf{r}')\cdot\boldsymbol{\nabla}_{\mathbf{r}'}\frac{\delta\mathcal{F}[\rho]}{\delta\rho(\mathbf{r}',t)}}_{\mathbf{j}_3}\Bigg\}. \quad (14)$$

Note that the first current density $\mathbf{j}_1$ in equation (14) is identical to the one in the original DDFT of Marconi and Tarazona [23,24] and persists when hydrodynamic interactions are neglected. $\mathbf{j}_2$ and $\mathbf{j}_3$ can be interpreted as the additional current densities due to the solvent-mediated interactions evoked by surrounding particles: $\mathbf{j}_2(\mathbf{r})$ describes the contribution of the solvent flow induced at position $\mathbf{r}$ reflected by neighboring particles at position $\mathbf{r}'$. The density current $\mathbf{j}_3(\mathbf{r})$ stems from the force acting at position $\mathbf{r}'$ mediated by the solvent. Both are weighted with the probability of finding particles at position $\mathbf{r}$ and $\mathbf{r}'$.

Finally, we need to close the above relation, which still depends on the two-body density. Within our approximation —the n-body densities are assumed to be identical to the equilibrium one of the reference system— it is given at every point in time by the exact generalized Ornstein-Zernike equation [35]:

$$\rho^{(2)}(\mathbf{r},\mathbf{r}',t) = \Big(1+c^{(2)}(\mathbf{r},\mathbf{r}')\Big)\,\rho(\mathbf{r},t)\rho(\mathbf{r}',t) + \rho(\mathbf{r}',t)\int \mathrm{d}\mathbf{r}''\Big((\rho^{(2)}(\mathbf{r},\mathbf{r}'',t)-\rho(\mathbf{r},t)\rho(\mathbf{r}'',t))c^{(2)}(\mathbf{r}'',\mathbf{r}')\Big), \quad (15)$$

with the Ornstein-Zernike direct correlation function

$$c^{(2)}(\mathbf{r},\mathbf{r}') = \frac{\delta^2\mathcal{F}_{\mathrm{exc}}[\rho]}{\delta\rho(\mathbf{r},t)\delta\rho(\mathbf{r}',t)}. \quad (16)$$

This implicit equation for the two-body density of the inhomogeneous system may be reasonably approximated by its bulk value [37,38], *i.e.* $\rho^{(2)}(\mathbf{r},\mathbf{r}',t)\approx\rho(r,t)\rho(r',t)g(|\mathbf{r}-\mathbf{r}'|,\bar{\rho})$, where $g(|\mathbf{r}-\mathbf{r}'|,\bar{\rho})$ is the pair correlation function for a homogeneous system at an appropriately averaged density $\bar{\rho}$, see footnote[1]. For a hard-sphere fluid, an analytic expression for the pair correlation function is available based on the Percus-Yevick equation [39].

To summarize, we derived a closed system of two equations that involve exclusively the equilibrium free-energy functional $F[\rho]$ to obtain the time evolution of the one-body density, including hydrodynamic interactions on the two-body level. Besides the approximation used for the equilibrium pair correlations, the only assumption in the derivation was that the out-of-equilibrium two-body and three-body densities are identical to those of an equilibrium system with the same instantaneous density. This assumption seems reasonable, since we consider overdamped Brownian dynamics, for which the momentum degrees of freedom relax instantaneously. This approximation is identical to assuming that the time evolution of the density would stop instantaneously if one actually switched on the additional potential $u(\mathbf{r},t)$, since then the density of the out-of-equilibrium system would be instantaneously identical to the equilibrium one and "only" the n-body densities, $n\geq 2$, would have to relax to their equilibrium values. This central assumption, sometimes referred to as *adiabatic approximation*, was first suggested by Marconi and Tarazona [24]. To date, a number of studies have demonstrated the accuracy of this approximation in a variety of different systems, see *e.g.* [20,25,27,28,32,40].

A final remark is that higher n-body hydrodynamic interactions can be treated analogously but lead to expressions that involve higher-equilibrium n-body densities of the reference system (compare Eq. (14)) and that a generalization of the theory to hard-sphere mixtures is straight forward.

3 Application to the dynamics of colloids in oscillating traps

We use the method presented above to predict the time evolution of the one-body density with hydrodynamic interactions by equation (14) for a cluster of $N = 100$ monodisperse spherical particles of diameter σ, whose interaction is hard, *i.e.*,

$$v_2(r_{ij}) = \begin{cases}\infty & \text{if } r_{ij}\leq\sigma,\\ 0 & \text{else,}\end{cases} \quad (17)$$

with $r_{ij} = |\mathbf{r}_i - \mathbf{r}_j|$. Henceforth, σ serves as the unit of length, the appropriate time scale is $\tau_{\mathrm{B}} = \sigma^2/D_0$, and the energy unit is $k_{\mathrm{B}}T$. The particles are trapped in a fixed spherical confining cavity which switches from a stable to an unstable shape periodically in time, see Figure 1. The explicitly time-dependent total external potential reads

$$V_{\mathrm{ext}}(r,t) = V_1\left(\frac{r}{R_1}\right)^4 + V_2\cos(2\pi t/\tau)\left(\frac{r}{R_2}\right)^2, \quad (18)$$

with $r = |\mathbf{r}|$. $R_1 = 4\sigma$ and $R_2 = \sigma$ are two length scales and $V_1 = 10k_{\mathrm{B}}T$ and $V_2 = k_{\mathrm{B}}T$ are the strengths of the two parts of the potential. This potential consists of a fixed cavity and a part which oscillates in time from a stable to an unstable cavity with a period $\tau = 0.5\tau_{\mathrm{B}}$. We assume that the effects of hydrodynamic interactions are most prominent for a period in this regime because in the limit of small τ particles barely move [27] and in the other limit for large τ the effect of hydrodynamic interactions should disappear (quasi-static process conduct). We have carried out additional simulations which show that different shapes of the external potential lead to the same qualitative behavior. A sketch of the setup is shown in Figure 1.

[1] We expect that in the stationary case the solution is the equilibrium solution even after this approximation, but we do not have a rigorous proof for this.

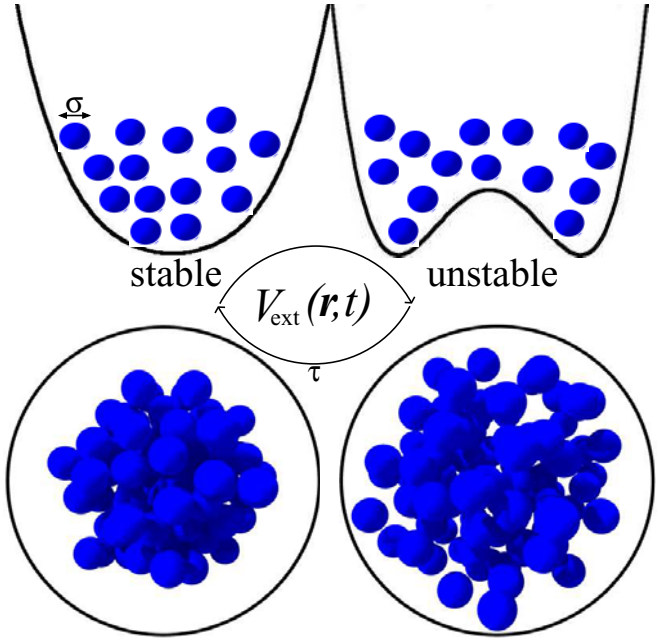

Fig. 1. (Color online) Sketch of the confined system. The external potential models an optical trap $V_{\rm ext}(r,t)$ which changes its central shape from stable to unstable within a time period τ. The trap confines N colloidal hard spheres of diameter σ shown as black circles. Additionally, typical 3d simulation snapshots are shown. The left-hand side shows an initial stable configuration for $t=0$ and the right-hand side shows an unstable situation at $t=2.75\tau_{\rm B}$ for case (N).

Due to the spherical symmetry, the density profile $\rho(r,t)$ depends on only one effective coordinate, namely the absolute value of the coordinate vector $r=|\mathbf{r}|$. The confining potential only acts on the colloidal particles while it is penetrable for the solvent molecules. Therefore, the solvent is treated as an unbounded fluid.

The pair correlation $g(|\mathbf{r}-\mathbf{r}'|,\bar{\rho})$ is calculated at each time step at the average density of the system $\bar{\rho}(t)=1/R_{\rm max}(t)\int_0^{R_{\rm max}(t)}{\rm d}r\rho(r,t)$, where $R_{\rm max}$ is defined by $V_{\rm ext}(r=R_{\rm max}(t))=10k_{\rm B}T$.

A crucial input to the DDFT is an accurate equilibrium excess free-energy functional. For a hard-sphere liquid, Rosenfeld's FMT [18] provides a very reliable approximation scheme for $\mathcal{F}_{\rm exc}[\rho]$. FMT is a generalized form of weighted-density approximations for fluids designed to model hard objects. The weighted densities are thereby obtained by convolutions with weight functions, where a spatial convolution is given by $g(\mathbf{r})*h(\mathbf{r})=\int{\rm d}\mathbf{x}\ g(\mathbf{x})h(\mathbf{r}-\mathbf{x})$. The weight functions reflect the geometrical properties of the constituent particles. For hard spheres they are given by

$$w_3(\mathbf{r})=\Theta(R-r),\quad w_2(\mathbf{r})=\delta(R-r), \tag{19}$$

$$\boldsymbol{w}_{\rm v2}(\mathbf{r})=w_2(\mathbf{r})\mathbf{r}/r,\quad \boldsymbol{w}_{\rm m2}(\mathbf{r})=w_2(\mathbf{r})[\mathbf{rr}/r^2-\mathbf{1}/3], \tag{20}$$

and the linearly dependent weights

$$w_1(\mathbf{r})=\frac{w_2(\mathbf{r})}{4\pi R},\quad \boldsymbol{w}_{\rm v1}(\mathbf{r})=\frac{\boldsymbol{w}_{\rm v2}(\mathbf{r})}{4\pi R},\quad w_0(\mathbf{r})=\frac{w_1(\mathbf{r})}{R}, \tag{21}$$

with the Dirac distribution $\delta(x)$, and the radius $R=\sigma/2$ of the spheres. **rr** denotes a dyadic product and **1** the 3×3 identity matrix. Convolution with the density $\rho(\mathbf{r})$ yields the weighted densities

$$n_\nu(\mathbf{r})=\rho(\mathbf{r})*w_\nu(\mathbf{r}),\quad \nu=3,2,1,0,{\rm v2},{\rm v1},{\rm m2}. \tag{22}$$

The excess free-energy functional is obtained by integrating over a free-energy density

$$\beta\mathcal{F}_{\rm exc}[\rho]=\int{\rm d}\mathbf{r}\ \Phi(\{n_\nu\}), \tag{23}$$

where the reduced free-energy density Φ is a function of the weighted densities n_ν and reads

$$\Phi=-n_0\ln(1-n_3)+\frac{(n_1n_2-\boldsymbol{n}_{\rm v1}\cdot\boldsymbol{n}_{\rm v2})}{(1-n_3)} +\frac{n_2^3/3-n_2\boldsymbol{n}_{\rm v2}^2+3(\boldsymbol{n}_{\rm v2}\boldsymbol{n}_{\rm m2}\boldsymbol{n}_{\rm v2}-3\det\boldsymbol{n}_{\rm m2})/2}{8\pi(1-n_3)^2}. \tag{24}$$

The contributions involving $\boldsymbol{n}_{\rm m2}$ are small and will be neglected henceforth. They were given here for completeness.

Since static DFT is derived for the grand-canonical ensemble, the question arises whether it is appropriate for a spherical cavity with a fixed number of particles. The densities obtained by static DFT correspond to a system with a chemical potential chosen such that the average number of particles $\langle N\rangle$ is equal to the number of particles within the cavity. This density profile is not necessarily the same as for the canonical ensemble. This issue was addressed by González and co-workers [41,42]. They showed that for a sufficient number of particles, $N>40$ say, the grand-canonical results are in very good agreement with the canonical ones. Therefore we conclude that the difference between different ensembles is negligible for our setup.

The last inputs to our theory are the tensors $\boldsymbol{\omega}_{11}(\mathbf{r}-\mathbf{r}')$ and $\boldsymbol{\omega}_{12}(\mathbf{r}-\mathbf{r}')$ that account for the hydrodynamic interactions between a pair of spheres. We approximate $\boldsymbol{\omega}_{12}(\mathbf{r}-\mathbf{r}')$ by the well-known Rotne-Prager expression [43]

$$\boldsymbol{\omega}_{12}(\mathbf{r})=\frac{3}{8}\left(\frac{\sigma_{\rm H}}{r}\right)[\mathbf{1}+\hat{\mathbf{r}}\hat{\mathbf{r}}]+\frac{1}{16}\left(\frac{\sigma_{\rm H}}{r}\right)^3[\mathbf{1}-3\hat{\mathbf{r}}\hat{\mathbf{r}}] +\mathcal{O}\left[\left(\frac{\sigma_{\rm H}}{r}\right)^7\right], \tag{25}$$

and neglect $\boldsymbol{\omega}_{11}(\mathbf{r}-\mathbf{r}')$, whose leading term is $\mathcal{O}((\sigma_{\rm H}/r)^4)$. On this level of approximation, we incorporate correctly all solvent-mediated interactions up to order $\mathcal{O}((\sigma_{\rm H}/r)^3)$ [44]. In our studies, we have chosen a hydrodynamic diameter of $\sigma_{\rm H}=3\sigma/4$, see footnote[2].

[2] For the validity of the far-field expressions for the hydrodynamic interactions used in this paper, it is important that particle stay sufficiently away from each other. Hence we have chosen the interaction hard-core diameter σ to be larger than the hydrodynamic diameter $\sigma_{\rm H}$. If these were equal, lubrication forces close to contact would involve more complicated near-field hydrodynamic tensors.

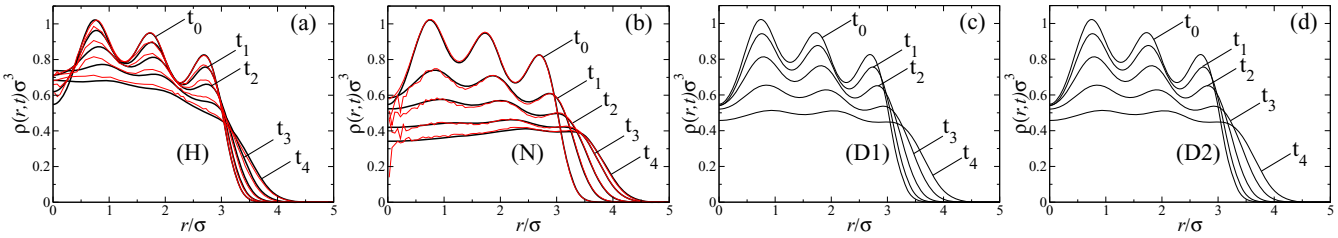

Fig. 2. (Color online) DDFT (solid curves) and BD (noisy curves) results for the time-dependent density profile $\rho(r,t)$ for the initial relaxation. In panel (a) hydrodynamic interactions are taken into account, in (b) they are neglected, in (c) and (d) they are included via the density-dependent diffusion coefficients in equation (27) and equation (28), respectively. The profiles correspond to the following time sequence: $t_0 = 0.0\tau_B$, $t_1 = 0.1\tau_B$, $t_2 = 0.15\tau_B$, $t_3 = 0.2\tau_B$, and $t_4 = 0.25\tau_B$.

The partial integro-differential equation governing the time evolution of $\rho(r,t)$, equation (14), is solved numerically employing a finite-difference approximation with a fixed time step of $10^{-5}\tau_B$.

The DDFT results are tested against Brownian dynamics simulations [45,46] performed on the same level of accuracy for the diffusion tensor, in which the hard interaction is approximated by a slightly softened one

$$\frac{v_2(r)}{k_BT} = \begin{cases} \left[\left(\frac{\sigma}{r}\right)^{48} - \left(\frac{\sigma}{r}\right)^{24} + \frac{1}{4}\right] & \text{if } r \le 2^{1/24}\sigma, \\ 0 & \text{else.} \end{cases} \quad (26)$$

In all simulations we chose a time step $10^{-4}\tau_B$. In order to obtain the time-dependent density $\rho(r,t)$ we perform a large number $N_{run} = 10^4$ of independent runs with different initial configurations sampled from a situation with a static external potential, *i.e.*, equation (18) at $t = 0$. Additionally, the densities are compared to those obtained by standard DDFT, where hydrodynamic interactions are ignored.

Finally we also compare our results to those obtained by conventional DDFT when hydrodynamic interactions are taken into account via a density-dependent diffusion coefficient [32]. This procedure makes use of an analytic expression for the reduction of the sedimentation velocity of hard spheres as a function of the hydrodynamic volume fraction $\phi_{HI} = \pi\rho/6\sigma_{HI}^3$ calculated by Hayakawa and Ichiki [47]. Their resulting equation consists of a far-field and a near-field lubrication term and reads

$$D(\phi_{HI})/D_0 = (1-\phi_{HI})^3/[1+2\phi_{HI}+1.492\phi_{HI}(1-\phi_{HI})^3]. \quad (27)$$

When the near-field term is neglected it reduces to

$$D(\phi_{HI})/D_0 = (1-\phi_{HI})^3/[1+2\phi_{HI}]. \quad (28)$$

As proposed in [32], we generalize to strongly inhomogeneous situations by using the local packing fraction $\bar{\phi}(r,t)$ calculated by convolving the bare density profile, $\rho(r,t)$, with a weight function characteristic of the particle volume, namely $\bar{\phi}(r,t) = n_3(r,t)(\sigma_{HI}/\sigma)^3$, where n_3 is given in equation (22).

4 Results

We now present the results obtained by DDFT and Brownian dynamics simulation for the setups introduced in the preceding section. The four different situations will be labeled henceforth as follows: the case of hydrodynamic interactions included via equation (14) (H), the case of hydrodynamic interactions ignored (N), and the cases of the two density-dependent diffusion coefficients with near-field hydrodynamic interactions (D1) and without near-field hydrodynamic interactions (D2), respectively. First of all, the associated profiles for $\rho(r,t)$ for the initial half-period in which the cavity is unstable are shown in Figure 2. The initial density profile is the equilibrium one for $V_{ext}(r, t = 0)$ in all four situations (H), (N), (D1), and (D2) which exhibits three correlation peaks in the density profile due to layering. Simulation data for simple Brownian dynamics and with included hydrodynamic interactions are also shown in Figure 2 (a) and (b), respectively, for the initial relaxation. One first important conclusion is that the theory describes the simulation data very well. If hydrodynamic interactions are more crudely taken into account via the (D1) or (D2) approach, the theory deviated considerably from the simulation data with hydrodynamic interactions (see Fig. 2). Qualitative features are, however, kept. As a second observation, we remark that hydrodynamic interactions damp the dynamics considerably and slow down the relaxation to the steady state. The steady-state itself is shown in Figure 3. The same qualitative conclusion as for Figure 2 hold regarding the quality of the theoretical approaches (H), (N), (D1), (D2) and the influence of hydrodynamic interactions in general.

A peculiar result is the dynamics of the central density $\rho(r = 0, t)$. Hydrodynamic interactions tend to push this quantity up upon expansion which is an unusual effect that is kept only within the (H) approach but is lost in (N), (D1), and (D2). This effect is even more pronounced in the initial relaxation, see Figure 2. We think that this behavior is due to particle fluctuations near the cavity center. If more particles are in one half of the cavity these are dragging nearby particle over the center and this gives rise to the increase of the central density as the cavity expands.

Figure 4 underlines the oscillating behavior into the steady state by showing the density at a fixed distance $r = 2.86\sigma$ from the cavity center, *i.e.* the position of the

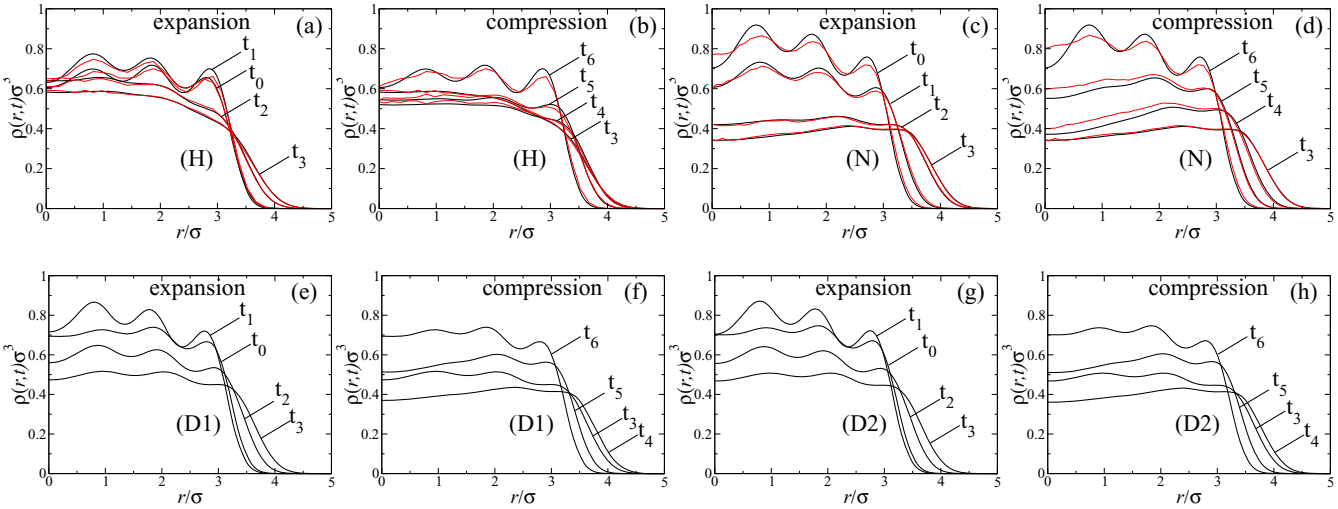

Fig. 3. (Color online) *Steady-state* DDFT (solid curves) and BD (noisy curves) results for the time-dependent density profile $\rho(r,t)$. Both half-periods for all situations are shown; hydrodynamic interactions taken into account via equation (14) (H), via a density-dependent diffusion constant with (D1) and without (D2) near-field hydrodynamic interaction, and hydrodynamic interaction ignored (N). The profiles correspond to the following time sequence: $t_0 = 2.5\tau_B$, $t_1 = 2.6\tau_B$, $t_2 = 2.7\tau_B$, $t_3 = 2.75\tau_B$, $t_4 = 2.85\tau_B$, $t_5 = 2.9\tau_B$, and $t_6 = 3.0\tau_B$.

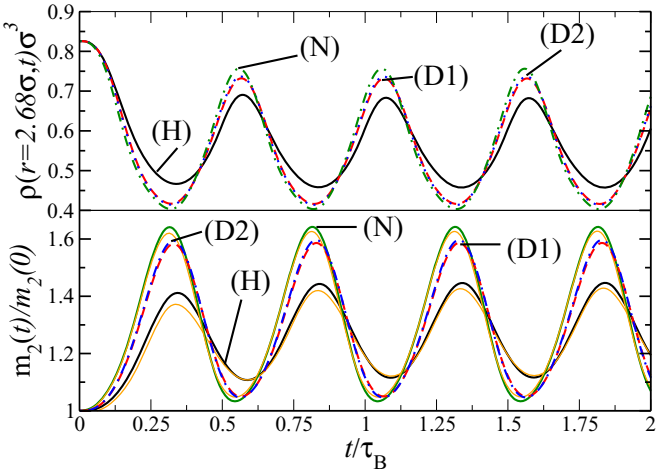

Fig. 4. (Color online) Top: oscillations at the position of the third peak in the initial density profile, *i.e.* for $r = 2.86\sigma$, of the system *versus* time. DDFT results with hydrodynamic interactions taken into account (H), being neglected (N), and taken into account via a density-dependent diffusion coefficient with (D1) and without (D2) near-field hydrodynamic interactions. Bottom: second moment of the density profile, $m_2(t)$, *versus* time t. DDFT (solid curves) and BD (noisy curves) with labeling as before.

third peak in the initial density profile. The damping is most pronounced for the approach (H).

We finally consider the second moment of the density, $m_2(t)$, defined through

$$m_2(t) = \int \mathrm{d}\mathbf{r}\; r^2 \rho(r,t). \tag{29}$$

This quantity is a measure of the spread of $\rho(r,t)$ around the center of the external field. Its time evolution is also depicted in Figure 4. Obviously, the time evolution of $m_2(t)$ for (H) and (N) is different and it also supports our earlier finding that the dynamics of the system with hydrodynamic interactions are considerably slowed compared to (N). System (N) is already in its steady state within the first period and correspondingly the second moment is virtually the same for the next periods. System (H) on the other hand, needs two periods to be in the steady state. Furthermore, Figure 4 reveals that the stable and the unstable half-period are asymmetric and not each other's "time reverse". Finally hydrodynamic interactions lead to a stronger phase shift with respect to the driving external potential.

5 Conclusions

In this paper, we have presented a dynamical density functional theory with hydrodynamic interactions incorporated on a two-particle level. As an application of the theory, we have studied a hard-sphere system in an optical trap which switches periodically from a stable to an unstable confining potential. The theory has been supplemented by an accurate equilibrium free-energy functional, namely Rosenfeld's FMT functional. We have found good agreement for the dynamical development of the density profile. By comparing the results to those obtained from conventional DDFT, where hydrodynamic interactions are ignored, we find significant differences. In particular, the time evolution is considerably slowed and oscillations in the steady-state density profile in the trap center are damped by hydrodynamic interactions.

The presented formalism provides a theory that can be applied to arbitrary time-dependent external potentials and systems, provided the applied external forces are moderate and an accurate equilibrium free-energy functional

is known. It would be interesting to study, *e.g.*, sedimentation or the onset of laser-induced freezing of colloids [48]. Also pure relaxational dynamics in a fixed (*i.e.* time-independent) external potential can be treated within the present approach and it would be interesting to study the influence of hydrodynamic interactions on the dynamics of freezing and vitrification in confinement, *i.e.* for hard spheres in hard spherical cavities [49]. It would be further challenging to generalize the present formalism to many-body interparticle interactions and many-body hydrodynamic interactions, to toroidal traps [50], and to anisotropic particles with orientational degrees of freedom. For the latter case the DDFT was derived from the Smoluchowski equation at least for the case of neglected hydrodynamic interactions [51].

Finally, Archer [30] has demonstrated how mode coupling theory, which is capable of predicting glass transition, can be brought in relation to DDFT for atomic liquids. It is tempting to use the above formalism to derive a mode coupling theory including hydrodynamic interactions since it is anticipated that hydrodynamic interactions play an important role in the dynamics near the hard-sphere glass transition [52].

We thank G. Nägele, M. Rauscher, A. Archer, C.F. Lee and C.P. Royall for helpful discussions. This work is supported by the DFG within SFB TR6 (project D3).

References

1. P.N. Pusey, in *Liquids, Freezing and Glass Transition*, edited by J.P. Hansen, D. Levesque, J. Zinn-Justin (North-Holland, Amsterdam, 1991).
2. E. Allahyarov, H. Löwen, Phys. Rev. E **63**, 041403 (2001).
3. E. Allahyarov, H. Löwen, J. Phys.: Condens. Matter **13**, L277 (2001).
4. M. Doi, S.F. Edwards, *The Theory of Polymer Dynamics*, 1st ed. (Clarendon Press, Oxford, 1986).
5. J.K.G. Dhont, *An Introduction to Dynamics of Colloids* (Elsevier Science, Amsterdam, 1996).
6. G. Nägele, J.K.G. Dhont, J. Chem. Phys. **108**, 9566 (1998).
7. G. Nägele, J. Bergenholtz, J. Chem. Phys. **108**, 9893 (1998).
8. G. Nägele, J. Bergenholtz, J.K.G. Dhont, J. Chem. Phys. **110**, 7037 (1999).
9. S. Harris, J. Phys. A: Math. Gen. **9**, 1895 (1976).
10. B.U. Felderhof, J. Phys. A: Math. Gen. **11**, 929 (1978).
11. G. Nägele, J. Phys.: Condens. Matter **15**, S407 (2003).
12. B. Cichocki, M.L. Ekiel-Jezewska, P. Szymczak, E. Wajnryb, J. Chem. Phys. **117**, 1231 (2002).
13. R. Pesché, G. Nägele, Europhys. Lett. **51**, 584 (2000).
14. R.A. Lionberger, W.B. Russel, J. Rheol. **41**, 399 (1997).
15. J.Z. Wu, AIChe J. **52**, 1169 (2006).
16. H. Löwen, Phys. Rep. **237**, 249 (1994).
17. Y. Singh, Phys. Rep. **207**, 351 (1991).
18. Y. Rosenfeld, Phys. Rev. Lett. **63**, 980 (1989).
19. Y. Rosenfeld, M. Schmidt, H. Löwen, P. Tarazona, Phys. Rev. E **55**, 4245 (1997).
20. A.J. Archer, J. Phys.: Condens. Matter **17**, 1405 (2005).
21. N. Grewe, W. Klein, J. Math. Phys. **18**, 1729; 1735 (1977).
22. C.N. Likos, A. Lang, M. Watzlawek, H. Löwen, Phys. Rev. E **63**, 031206 (2001).
23. U.M.B. Marconi, P. Tarazona, J. Phys.: Condens. Matter **12**, A413 (2000).
24. U.M.B. Marconi, P. Tarazona, J. Chem. Phys. **110**, 8032 (1999).
25. A.J. Archer, R. Evans, J. Chem. Phys. **121**, 4246 (2004).
26. F. Penna, J. Dzubiella, P. Tarazona, Phys. Rev. E **68**, 061407 (2003).
27. M. Rex, C.N. Likos, H. Löwen, J. Dzubiella, Mol. Phys. **104**, 527 (2006).
28. M. Rex, H. Löwen, C.N. Likos, Phys. Rev. E **72**, 021404 (2005).
29. G.K.L. Chan, R. Finken, Phys. Rev. Lett. **94**, 183001 (2005).
30. A.J. Archer, J. Phys.: Condens. Matter **18**, 5617 (2006).
31. A.J. Archer, M. Rauscher, J. Phys. A: Math. Gen. **37**, 9325 (2004).
32. C.P. Royall, J. Dzubiella, M. Schmidt, A.V. Blaaderen, Phys. Rev. Lett. **98**, 188304 (2007).
33. M. Rex, H. Löwen, arXiv:0803.2009 [physics].
34. G. Nägele, *Lecture notes* (Institut of Fundamental Technological Research, Polish Academy of Science, Warsaw, Poland, 2004).
35. R. Evans, Adv. Phys. **28**, 143 (1979).
36. J.P. Hansen, I.R. MacDonald, *Theory of Simple Liquids*, 3rd ed. (Academic, London, 2006).
37. S. Dietrich, A. Haase, Phys. Rep. **260**, 1 (1995).
38. B. Götzelmann, A. Haase, S. Dietrich, Phys. Rev. E **53**, 3456 (1996).
39. A. Trokhymchuk, I. Nezbeda, J. Jirsák, D. Henderson, J. Chem. Phys. **123**, 024501 (2005).
40. J. Dzubiella, C.N. Likos, J. Phys.: Condens. Matter **15**, L147 (2003).
41. A. González, J.A. White, F.L. Román, S. Velasco, R. Evans, Phys. Rev. Lett. **79**, 2466 (1997).
42. A. González, J.A. White, F.L. Román, R. Evans, J. Chem. Phys. **109**, 3637 (1998).
43. J. Rotne, S. Prager, J. Chem. Phys. **50**, 4831 (1969).
44. S. Kim, S.J. Karrila, *Microhydrodynamics: Principles and Selected Applications* (Butterworth-Heinemann, Boston, 1991).
45. M.P. Allen, D.J. Tildesley (Editors), *Computer Simulation of Liquids* (Clarendon Press Oxford, Oxford, 1989).
46. D.L. Ermak, J.A. McCammon, J. Chem. Phys. **69**, 1352 (1978).
47. H. Hayakawa, K. Ichiki, Phys. Rev. E **51**, R3815 (1995).
48. A. Chowdhury, B.J. Ackerson, N.A. Clark, Phys. Rev. Lett. **55**, 833 (1985).
49. Z.T. Nemeth, H. Löwen, Phys. Rev. E **56**, 6824 (1999).
50. C. Lutz, M. Reichert, H. Stark, C. Bechinger, Europhys. Lett. **74**, 719 (2006).
51. M. Rex, H. Löwen, Phys. Rev. E **75**, 051402 (2007).
52. M. Tokuyama, Rep. Inst. Fluid Sci. **19**, 7 (2007).